HAL
open science

3D modelling of electrostatic force distance curve between the AFM probe and dielectric surface

Abderrhramane Boularas, Fulbert Baudoin, G. Teyssedre, Christina Villeneuve-Faure, Stéphane Clain

To cite this version:

Abderrhramane Boularas, Fulbert Baudoin, G. Teyssedre, Christina Villeneuve-Faure, Stéphane Clain. 3D modelling of electrostatic force distance curve between the AFM probe and dielectric surface. 9e Conférence Société Française d'Electrostatique (SFE), Toulouse, France, 27-29 Aout 2014, Aug 2014, Toulouse, France. pp. 407-412. hal-03034537

HAL Id: hal-03034537

https://hal.science/hal-03034537v1

Submitted on 1 Dec 2020

HAL is a multi-disciplinary open access archive for the deposit and dissemination of scientific research documents, whether they are published or not. The documents may come from teaching and research institutions in France or abroad, or from public or private research centers.

L'archive ouverte pluridisciplinaire **HAL**, est destinée au dépôt et à la diffusion de documents scientifiques de niveau recherche, publiés ou non, émanant des établissements d'enseignement et de recherche français ou étrangers, des laboratoires publics ou privés.

3D modelling of electrostatic force distance curve between the AFM probe and dielectric surface

A. Boularas[1*], F. Baudoin[1], G. Teyssedre[1], C. Villeneuve-Faure[1], S. Clain[2, 3]
[1] Laboratoire Plasma et Conversion d'Energie - LAPLACE
Bât. 3R3, 118 route de Narbonne, 31062 Toulouse Cedex, France
[2] Université du Minho, DMA et CMAT, Campus d'Azumè, Guimarães, Portugal
[3] Université Paul Sabatier, Institut de mathématique de Toulouse, Toulouse, France
* E-mail : boularas@laplace.univ-tlse.fr

Abstract: Techniques derived from the near-field microscopies and particularly the Atomic Force Microscopy (AFM) are presented as alternative techniques for measurement of space charge compared to classical techniques due to their high sensitivity to the electrostatic force and a better resolution (≈ nm). One of the AFM derivative techniques which allow obtaining information on the charge state of the dielectric materials is based on the technique of Force Distance Curves (FDC) obtained by cycle of approach and retracts between the AFM probe and the dielectric. In this paper, three-Dimensional (3D) simulation results for the electrostatic force between an Atomic Force Microscope (AFM) tip and the surface of a dielectric are presented for different AFM tip geometries. The first aim is to analyse the effect of the geometric parameter on force-distance curves without contribution of the cantilever as AFM detection mode for electrostatic charges. At the second time the sensor is composed of a cantilever supporting a conical tip terminated by a spherical apex, we investigate in a second step is to see the effect of the cantilever on force distance curve. Simulation results are shown and compared with experimental data in order to validate our approach.

INTRODUCTION

The study of solid dielectric materials, especially injection phenomena and charge accumulation is still a very important challenge for the reliability of electrical systems. Several techniques for measuring space charge are available: pulsed electroacoustic –PEA– methods [1], thermal methods (Laser Induced Modulation Method –LIMM– or Thermal Pulse –TP–) [2] but they are still limited in their spatial resolution (≈ micrometre), for the study of insulating films of small thickness as can be found in electronic components with thicknesses of the order 10- 50 nm. Meanwhile, techniques derived from the near-field microscopy [3] such as Atomic Force Microscopy (AFM) [4] and the derivative techniques such as Kelvin Force Microscopy (KFM) [5-7] and Force Distance Curve (FDC) [8, 9] have appeared. Our purpose here is to exploit near field techniques derived from Atomic Force Microscopy (AFM) which appears as invaluable tools for nanometer scale materials diagnostic [10, 11].

These techniques allow us to have information on the state of charge of insulation and their ability to store / dissipate these charges; the KFM is used to measured surface potential modification induced by charges. However vertical localization of charges seems difficult to attempt, EFDC (Electrostatic Force Distance Curve) follows electrostatic force evolution as function of tip-surface separation distance. This technique, based on FDC, appears promising because of its high resolution, sensitivity to charges localization and distance dependence. Measurements of EFDC and surface potential are available [12], but the quantitative interpretation of the results obtained requires the use of modelling. Modeling KFM electrostatic conditions remains difficult, due to the oscillating nature of the technique. Simplification of the problem is expected through direct study of the evolution of the electrostatic force induced by trapped charges. Therefore the objective of our study is to develop a numerical model to do a metrological analysis of the AFM probe with the force curves. To do this study, a three dimensional electrostatic model was developed with commercial software Comsol Multiphysics®. Several geometries of the AFM tip were tested: cone, pyramid and tetrahedron. These simulations help us to establish what geometry of the AFM tip will give us the results closest to that of the measurement. On the other hand, an analysis of the different parts of an AFM probe was performed to estimate the contribution of each element of the probe on the curve shape. A three-dimensional electromechanical model was also developed; the cantilever and tip are considered in this model. The coupling of the two studies, electrostatic and mechanical allows us to evaluate the effect of the contribution of the cantilever to the results of force curve. The force curve is obtained by gradually increasing the tip / sample distance, the force is estimated by deflection of the AFM probe.

The paper is structured as follows: in section 2 we describe the probe-thick insulator substrate system where we use to compute a force distance curve approximation between tip and sample with the three-dimensional electrostatic model. Poisson equation is solved using FEM to provide the electrical potential and electric field, the electrostatic force here is

calculated using the Maxwell-stress-tensor. In section 3 we analyse how the kind of geometry of the AFM tip influance the tip-substrate electrostatic interaction and force distance curve. In section 4 we analyse the contribution of cantilever in the force distance curve by the three-dimensional electromechanical model, the electrostatic force here is estimate by the deflexion of cantilever Δz. The result of this simulation result is compared each time with the experimental result. Finally in section 5 we summarize the main conclusions of the paper.

ELECTROSTATIC FORCE DISTANCE CURVE

The technique of Force Distance Curve (FDC) permits direct measurement of interaction forces between the AFM tip and surface of sample. It is possible to isolate the electrostatic interaction, it by to exploiting the sensitivity of electrostatic forces when the AFM tip is biased or in presence of space charges in the sample. This sensitivity has been demonstrated elsewhere [13-15].

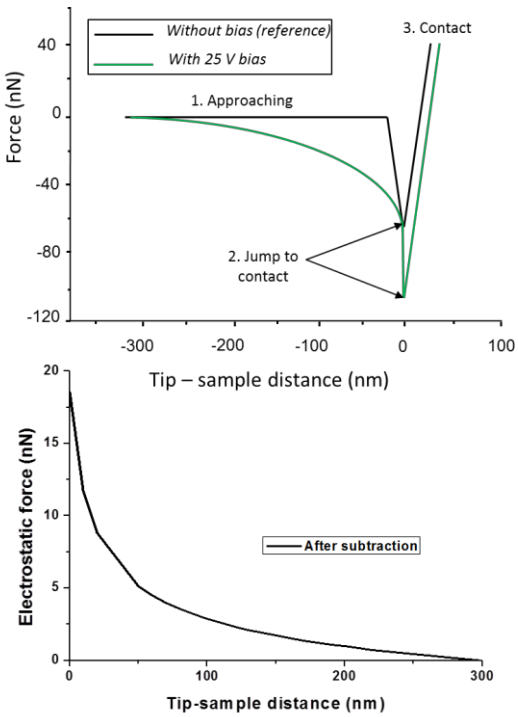

FIG.1 Electrostatic force vs. sample distance separation. A effect of applied voltage at the AFM tip; black curve represent the FDC without voltage at tip (reference) and green curve represent curve with voltage at tip. Subtracting the green curve and the reference curve provides the Electrostatic Force Distance separation Curve.

The electrostatic interactions are difficult to handle as they depend on the very geometry of the set-up and act over long distances: this leads to problems for building a realistic model. Therefore some simplified model system is used to describe the complex AFM setup. In general a sample is assumed to be flat and the geometry of the AFM tip is assumed as a conical tip with cylindrical symmetry. The most used shapes found in the literature are: A simple charge [16] a sphere [17] or a cone [18] where a metallic tip and flat sample are assumed. The important case of dielectric is seldom treated due to its complexity, as image-charge method in thick dielectric film [19]. The numerical modelling of forces [20-22] is in accordance with experiments except for small tip to sample distances [23]. Most of this study is mainly focused on the influence of experimental conditions (tip characteristic, velocity…) on the force. However, from the experimental point of view no systematic study of electrostatic force has been performed and theoretically, no 2D or 3D models are available in order to quantify the charges density. The EFDC method consists in exploiting electrostatic sensitivity of the FDC. For this, two approaches of the AFM tip and the surface of the sample are made. As shown on Fig.1 (a) the first approach is with the bias applied on the tip and in the second one the tip is connected to the ground and it is considered as reference curve.Three main parts can be identified on each curve when the tip approaches the surface: 1- Tip approaches the surface, 2- Jump to contact (Van der Waals forces) and 3- Contact. As the electrostatic force is a long range force, the potential difference between tip and surface mainly modifies the approach behaviour (part 1 of the curve) without modifying the other steps. Thus, the electrostatic force can be extracted form the difference between force curve with and without potential. Fig. 1 (b) shows the resulting electrostatic force as function of tip-sample distance for 25V applied bias on the conductive tip.

THEORECAL MODELLING

To study the effect of the nanometre-scale parts of the AFM probe (the cone and the cantilever) on the electrostatic force interaction, we present in this paper several kinds of models. Let us consider the probe-sample system sketched in Fig. 2. In a first step we consider the simplified model with no consideration of the cantilever effect. The tip consists of a truncated cone of height L and cone aperture angle α ending with a semi-spherical apex radius R_c, (all geometric parameters are given in table 1).

TABLE 1. ELECTRICAL MATERIAL PROPERTIES AND GEOMETRICAL PARAMETER USED IN FEM MODELS

Term	Definition	Value
ε_r	Relative permittivity	4.35
R_c	Sphere radius	32 nm
D	Separation distance	0 – 400 nm
U	Potential difference	20 V
α	Cone half aperture angle	20°
L	Length of tip	10 µm
e	sample thickness	200 nm
l	diameter of the domain Ω	40 µm

This first model will give us the first results of force curve. After that we replace the truncated cone with the tip in the form of a pyramid and tetrahedral shape. These entire tips are positioned at the distance D of the insulating sample with the thickness e, and the sample is assumed to be flat. The insulating sample chosen here is SiON; the Pulsed plasma-enhanced chemical vapor deposition (PPECVD) was used as deposition technique to elaborate the dielectric layers. The ratio γ between the N_2O/SiH_4 gas fluxes allows adjusting the silicon content in the film. When decreasing the γ-value the Si content in the layer increases (process details are given in [24]).

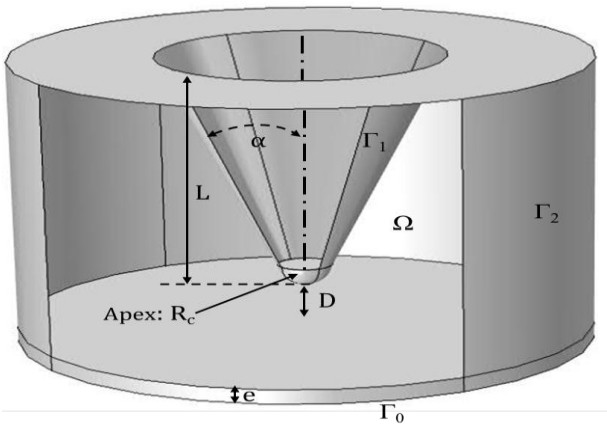

FIG.2 Sketch of the geometric representation and parameters of the tip-thick insulator system used in electrostatic three-dimensional finite-element numerical calculation in domain Ω.

In order to solve numerically the electrostatic problem in domain Ω, we use the finite-element package COMSOL Multiphysics® 4.0 and more exactly the AC/CD electrostatic module. Domain Ω is chosen large (40 µm) enough to neglect edge effects and obtain a relevant approximation to the problem of single point in front of an infinite plane in infinite space. It is chosen with a cylindrical box shape for the conical tip and cubic box shape for the AFM tip with pyramidal and tetrahedral shape. Poisson equation (1) is applied to the domain Ω of boundary Γ.

$$div\,(\varepsilon\ \mathbf{grad}\ (U)) = 0 \qquad (1)$$

where ε is the space-dependent relative permittivity for the sample and the gas. Interface Γ is decomposed into constant potential boundary Γ_0 at the bottom of the insulating substrate (here taken as ground) and Γ_1 on the probe surface, while Neumann boundary conditions Γ_2 were used on the lateral sides and the upper side of the simulation box (see Fig. 2). The electric field is derived from the potential:

$$\mathbf{E} = -\mathbf{grad}\ U \qquad (2)$$

The electric field Fig.3 (b) is the crucial parameter governing the near-field microscopy [25] and it is very sensitive to the radius of curvature of the AFM tip [13]. Therefore we are able to compute the electrostatic force acting on the probe function of the tip substrate separation distance by integration of the built-in Maxwell-stress-tensor (Mt) (3) aver all faces of the tip.

$$Mt = \frac{\varepsilon_0}{2}\left\|E\right\|^2 \qquad (3)$$

$$\mathbf{F}_e = \int_{\Gamma_1} Mt\,ds \qquad (4)$$

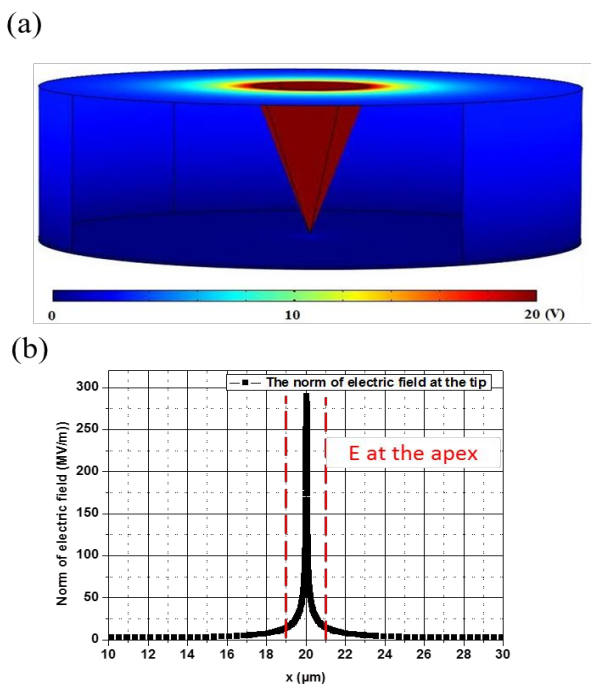

FIG.3 (a) Electric potential distributions created by the PtIr coated tip (R_c = 32 nm α = 20°, D = 100 nm and e = 200 nm) in front of dielectric simulated by three-dimensional FEM COMSOL Multiphysics®. (b) Electric field recorded over the surface of the tip. The thick insulator substrate has a dielectric constant ε_r = 4.35. The AFM tip is at 20 V while the backside of the substrate is at ground 0 V.

We estimated the accuracy of our calculations to be better than 1% against the analytical expression of the electrostatic force acting on a conducting sphere in front of an infinite dielectric substrate [26].

EFFECT OF TIP GEOMETRY ON THE ELECTRODTATIC FORCE SEPARATION DISTANCE CURVE

We are now going to present the results of the study of the Electrostatic Force Distance separation Curve EFDC. The aim here is to evaluate the impact of different

geometrical forms on electrostatic interaction between the AFM tip and the thick insulator. The tip chosen for this study is the PtIr coated probe with radius curvature R_c = 32 nm; other parameters are given in Tab.1. Fig. 3 shows the distribution of electric potential at the separation distance D = 100 nm, and the electric field recorded at the surface of the tip at the same distance D. To simulate the force separation curve we varied the distance D between 0 and 400 nm.

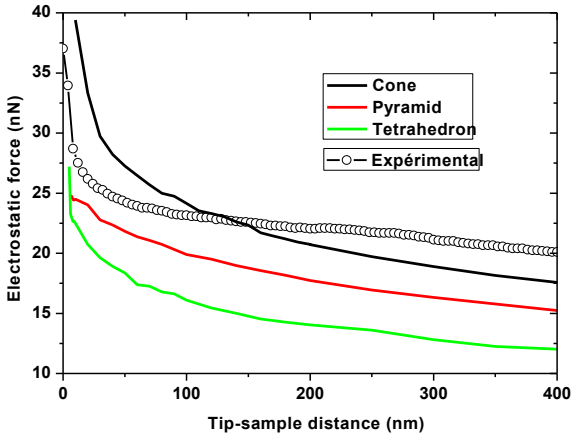

FIG.4. Electrostatic force versus distance separation between the AFM tip and sample for different tip geometry forms with the same geometry parameters, Apex radius R_c = 32 nm and cone half angle α = 20°. Comparison between results obtained by finite element method and experimental results, 20 V bias at the surface of the AFM tip.

The development of the three-dimensional model allows studying the influence of the geometry of the AFM tip on the results of the force curve in order to come most close to the real shape of the AFM tip, Fig. 5. The most difficult task here is using three-dimensional (3D) solver with large geometries including nanometric features (here the apex).

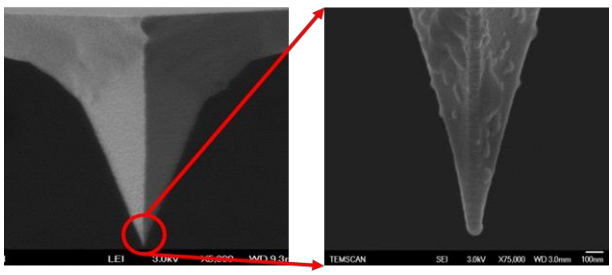

FIG.5 SEM image of the real AFM tip used in the experiment.

For this, three geometries are tested; the first one represents the tip with the cone and it is the most used in the literature. In the second step the tip is represented with the pyramidal shape and the last we used the tip with the tetrahedral shape. In Fig. 5 we present the comparison between the simulation results obtained by our FEM model on the different shape of the AFM tip with the experimental results of the force distance separation curve. The first observations show that the experimental results are in good correlation with simulation data obtained by the model with the tetrahedral shape of the AFM tip (green curve) Fig. 4. The tip with the cone shape overestimates on the values of the force. The result obtained by tip with pyramidal shape is close to experimental result but the curvature of the EFDC curve is not respected. An offset of the electrostatic force appears between the simulated data and experience. This shift is due to the fact that this model does not take into account the effect of the cantilever in the calculation of electrostatic force.

In summary we have shown that the result of force distance separation curve is sensitive to the shape of the AFM tip, and the tip with the tetrahedral shape shows results nearest to experimental results. The shift is due to the fact the model does not take into account the contribution of the cantilever.

EFFECT OF CANTILEVER ON THE ELECTRODTATIC FORCE SEPARATION DISTANCE CURVE

According to the result presented in section 3, the characteristic of nanometric geometry of the AFM tip need to be taken into account in any geometrical model used to characterize the Electrostatic Force Distance separation Curve EFDC. In this section we present the three-dimensional electromechanical model in order to analyze the effect of the second part on the AFM probe, the cantilever, in the Electrostatic Force Distance separation Curve EFDC.

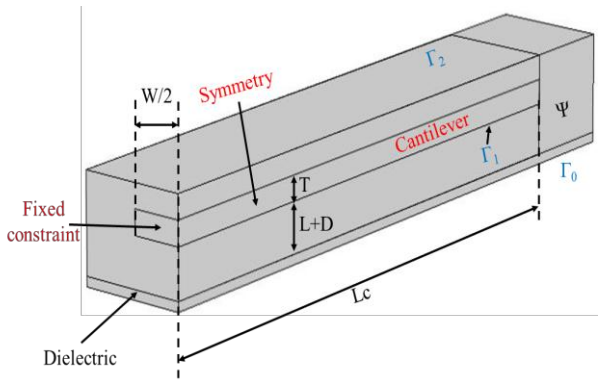

FIG.6 Sketch of the geometric representation and parameters of the cantilever-thick insulator system used in electromechanical three-dimensional finite-element numerical calculation in domain Ψ.

TABLE 2. GEOMETRICAL PARAMETER PROPERTIES OF CANTILEVER USED IN FEM MODELS (DATA SHEET)

Probe	material	*k* *(N/m)*	T (µm)	Lc (µm)	W (µm)
SCM-PIT	PtIr	2.8	2.75	225	28

The cantilever is modeled as a beam as shown in Fig. 6 and it is positioned at the distance L (the height of tip) + D (separation distance between tip and sample) see table 1. The cantilever is characterized by several geometric parameters detailed in Table 2. It is also characterized by the *k* spring constant which can be calculated by the equation (5):

$$k = \frac{E.W.T^3}{4.L^3} \quad (5)$$

where E is the Young's modulus, other parameters are taken from table 2. In order to solve numerically the electromecanic problem in domain Ψ, we use also the finite-element package COMSOL Multiphysics®. The domain Ψ is chosen large enough to neglect edge effects and obtain a relevant approximation of the problem. This domain is chosen with a cubic box shape in order to be able to mesh the domain with a regular mesh. Two important equations are solved in this model; the first one is Poisson equation (1) applied to the domain Ψ of boundary Γ detailed in Section 3. Interface Γ is decomposed into constant potential boundary Γ_0 on the bottom of the insulating substrate (here taken as ground) and Γ_1 on the surface of the cantilever, while Neumann boundary conditions Γ_2 were used on the lateral sides and the upper side of the box simulation (see Fig. 6). The second one is the mechanical equation which calculates the displacement force in the stationary case:

$$\nabla.\sigma = F_v \quad (6)$$

Where σ is the stress tensor and F_v is the forces exerted on the volume. The stress tensor must be continuous across a stationary boundary between two materials.

$$n_1(\sigma_2 - \sigma_1) = 0 \quad (7)$$

where σ_1 and e σ_2 represent the stress tensor in materials 1 and 2, respectively, and n_1 is the normal pointing out from the domain containing material 1. The mechanical boundary conditions are presented with fixed constraint in the left side of the cantilever and the symmetry condition in the face of geometry (See Fig. 6).

$$F_e = k.\Delta z \quad (8)$$

Where *k* is the spring constant and Δz is the displacement. At this step it is possible to estimate the influence of the cantilever in Electrostatic Force Distance separation Curve EFDC, by variying the distance D between 0 and 400 nm. The result of this curve is presented in Fig. 8 (a) it is compared to the result of force curve of the tip. Results show that the force created by the cantilever induces a very important force compared to the experimental EFCD.

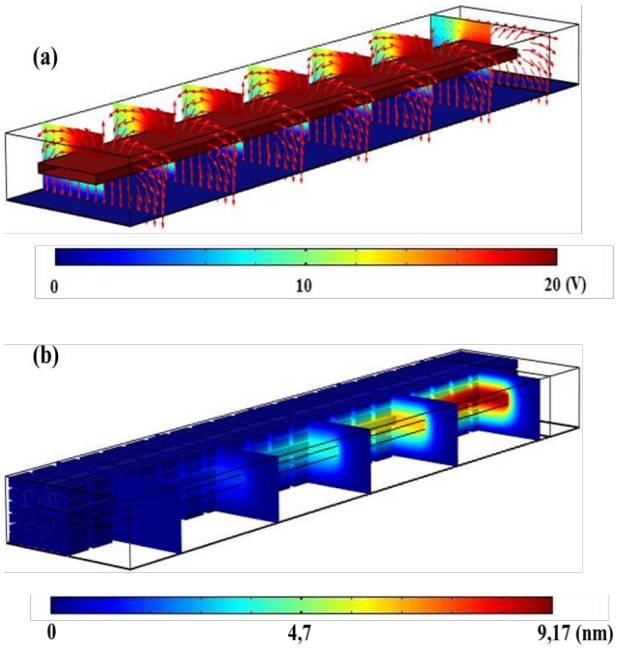

FIG.7 (a) Electric potential distributions and electric field vector created by the PtIr coated cantilever in front of dielectric simulated by three-dimensional FEM COMSOL Multiphysics®. (b) Displacement of the cantilever due to the deflection caused by the electrostatic force. The thick insulator substrate has a dielectric constant of ε_r = 4.35. The AFM cantilever is at 20 V and D=100nm while the backside of the substrate is at ground 0 V.

This feature is probably due to:

- the physical properties of the cantilever. Some studies show that the thickness of the cantilever, parameter T, plays an essential role on the force. Fig. 8 (b) shows the EFCD obtained with T = 3.5 µm instead of 2.75 µm as indicated by the data sheet. With this value, the EFCD is closed to the experimental data;
- the shape of the cantilever. It would be interesting to simulate the force created by the cantilever with geometry without singularity, in this case the cantilever is not a perfect parallelepiped but with the curved angles.

(a)

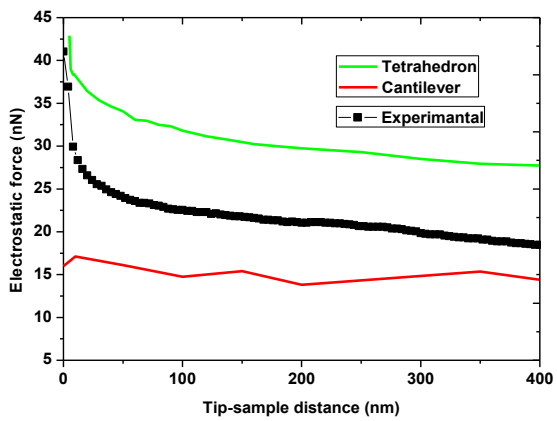

(b)

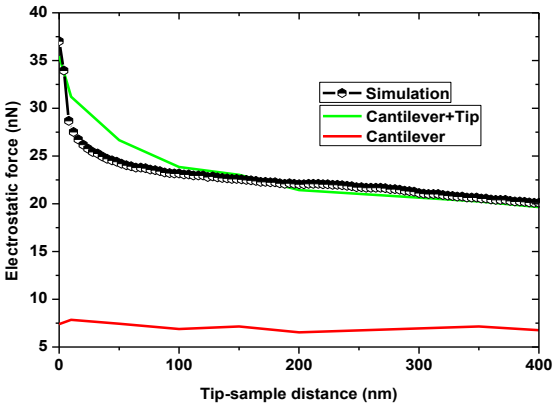

FIG.8 Electrostatic force versus distance separation between the AFM tip and sample for different tip geometry forms with the same geometry parameters, Apex radius R_c = 32 nm and cone half angle α = 20 °. Comparison between results obtained by finite element method FEM and experimental results, 20 V bias at the surface of the AFM cantilever, With (a) T=2.75 µm, (b) T=3.5 µm.

We note that the force curve due to the cantilever adds a constant force (red curve in Fig. 8). This contribution is added to the tip contribution, green curve in Fig. 8, in order to make a complete comparison of the force curve with the experimental results.

CONCLUSION

Two models have been developed in order to well understand the principle of electrostatic force measurement by AFM. This work focuses on the study of electrostatic force curve induced between two parts: the AFM probe and a flat dielectric sample. With the electrostatic model we could see the influence of the geometry of the tip on the curve electrostatic force. Electromecanical model has been used to evaluate the influence of the cantilever on the force curve. The results exhibit good qualitative and quantitative fit to experimental data, which allowed us to validate our approach. Results also highlight the fact that the radius of the tip plays an essential role on the value of the electrostatic force.

ACKNOWLEDGMENT

This work was supported by Region Midi-Pyrénées (France), by FEDER Funds through COMPETE Program and by Fundação para a Ciência e a Tecnologia (Portugal), within the Project PEst-C/MAT/UI0013/2011.

REFERENCES

[1] T. Maeno and K. Fukunaga, "High-resolution PEA charge distribution measurement system", IEEE Trans. Dielectr. Electr. Insul., vol. 3, p.754, (1996).

[2] S. B. Lang, "Laser intensity modulation method (LIMM): Experimental techniques, theory and solution of the integral equation" Ferroelectrics, vol. 118, pp. 343 - 361, (1991).

[3] G. Binnig, H. Rohrer, Ch. Gerber, and E. Weibel, "Surface Studies by Scanning Tunneling Microscopy" Phys. Rev. Lett., vol. 49, pp. 57–61, (1982)

[4] G. Binnig, C.F. Quate, and Ch. Gerber, "Atomic Force Microscope" Phys. Rev. Lett., vol. 56, p.930, (1986).

[5] C.A. Rezende et al. "Detection of charge distribution in insulator surfaces", J. Phys.: Condens. Matter 21, 263002 (2009)

[6] M. Ishii, "Static states and dynamic behaviour of charges: observation and control by scanning probe microscopy", J. Phys.: Condens. Matter 22, 173001 (2010)

[7] L. Borowik et al., "Calculating Kelvin force microscopy signals from static force fields", Appl. Phys. Lett. 96, 103119 (2010).

[8] B. Cappella and D. Dietler, "Force-distance curves by atomic force microscopy", Surf. Sci. Rep. 34, 1–104 (1999)

[9] S. Gomez, et al., "Electrostatic forces between sharp tip and metallic and dielectric surface", Appl. Phys. Lett. 79, 24 (2001)

[10] R. K. Leach et al., "The European nanotechnology landscape", Nanotechnology 22, 062001, (2011)

[11] H.N. Hansen et al., Ann. CIRP 55/2, 721, (2006)

[12] C. Villeneuve-Faure et al., "Kelvin force microscopy characterization of charging effect in thin a-SiO x N y :H layers deposited in pulsed plasma enhanced chemical vapor deposition process by tuning the Silicon-environment" J. Appl. Phys. 113, 204102 (2013)

[13] A. Boularas et al., "Multi-dimentional modelling of electrostatic force between atomic force microscopy tip and dielectric surface" IEEE ICSD, 1040-1043, (2013).

[14] S. Patil et al., "Investigation in the electrostatic forces in scanning probe microscopy at low bias voltage", Surf. Interface Anal. 33, 155 (2002).

[15] Y. Kim, et al., "Dependance of approaching velocity on the Force-Distance curve in AFM", Korean J. Chem. Engg. 27, 324 (2010).

[16] J. Hu, X.D. Xiao, and M. Salmerón, "Scanning polarization force microscopy: A technique for imaging liquids and weakly adsorbed layers" Appl. Phys. Lett., vol. 67, p. 476, (1995)

[17] B.D. Terris, J.E. Stern, D. Rugar, and H.J. Mamin, "Contact electrification using force microscopy" Phys. Rev. Lett., vol. 63, p. 2669, (1989).

[18] S. Beladi, P. Girard, and G. Leveque, "Electrostatic forces acting on the tip in atomic force microscopy: Modelization and comparison with analytic expressions" J. Appl. Phys., vol.81, p.1023, (1997).

[19] S. Gómez-Moñivas, L.S. Froufe-Pérez, A.J. Caamaño, and J.J. Sáenz, "Electrostatic force between sharp tips and metallic and dielectric sample", Appl. Phys. Lett., vol. 79, 4048, 2001.

[20] J. Colchero, A. Gil, and A. M. Baro "Resolution enhancement and improved data interpretation in electrostatic force microscopy" Phys. Rev. B, vol.24 , 245403, (2001)

[21] S. Blaidi, F. Lebon, P. Girard, G. Leveque, S. Pagano, "Finite element simulations of the resolution in electrostatic force microscopy", Appl. Phys. A, vol. 66, pp. S239-S243, (1998).

[22] T.S. Gros et al, "Two-dimensional, electrostatic finite element study of tip-substrate interactions in electric force microscopy of high density interconnect structure", Ultramicroscopy 87, 147 (2001)

[23] K. Makasheva, B. Despax, L. Boudou and G. Teyssedre, "Dielectric Layers for RF-MEMS Switches: Design and Study of Appropriate structure Preventing Electrostatic Charging" Electr. Insul. 19, 1195–1202 (2012)

[24] K. Makasheva, B. Despax, L.Boudou and G. Teyssedre "Dielectric Layers for RF-MEMS Switches: Design and Study of Appropriate Structures Preventing Electrostatic Charging" IEEE Trans. Dielectr. Electr. Insul., vol. 19, pp.1195-2002, 2012.

[25] S. Watanabe, H. Hane, T. Ohye, M. Ito, and T. Goto "Electrostatic force microscope imaging analyzed by the surface charge method", J. Vac. Sci. Technol. B, vol. 11, p. 1774, 1993.

[26] Smythe R 1968 Static and dynamic electricity 5new York: McGraw-Hill.

[27] A. Matthew et al.; "What is the Young's modulus of Silicon" J. Microelectromecanical system; Vol 19, No 2, (2010)